

**RESEARCH ARTICLE**

# Design and synthesis of boron complexes as new Raman reporter molecules for sensitive SERS nanotags

Rashid Javaid<sup>1</sup> | Nima Sayyadi<sup>1,2</sup> | Kausala Mylvaganam<sup>1</sup> |  
Koushik Venkatesan<sup>1</sup> | Yuling Wang<sup>1</sup> | Alison Rodger<sup>1</sup> <sup>1</sup>Department of Molecular Sciences,  
Macquarie University, Sydney, New South  
Wales, Australia<sup>2</sup>ARC Centre of Excellence for Nanoscale  
Bio photonics (CNBP), Macquarie  
University, Sydney, New South Wales,  
Australia**Correspondence**Alison Rodger, Department of Molecular  
Sciences, Macquarie University, Sydney  
2109, NSW, Australia.  
Email: alison.rodger@mq.edu.au**Funding information**Macquarie University, Grant/Award  
Number: iMQRES award scholarship**Abstract**

A new series of boron complexes consisting of pyridine-pyrazole ligands has been designed, synthesized and evaluated for its Raman activity using solid-state Raman spectroscopy. The detailed surface-enhanced Raman scattering (SERS) study of selected dye 2-(3-(pyridin-4-yl)-1H-pyrazol-5-yl) pyridine (P<sub>4</sub>) on gold nanoparticles (AuNPs) of size 40 nm revealed that it can detect as small as the nanomole level with signal quality that is superior to structurally similar commercially available reporter molecules (RMs), rendering it a suitable RM for sensitive SERS nanotags.

**KEYWORDS**

boron complexes, molecular design, pyridine, Raman reporter, SERS

## 1 | INTRODUCTION

Surface-enhanced Raman scattering (SERS) has been explored extensively during the last decade due to its potential as an alternative to commonly used fluorescence methods for biological sensing.<sup>[1–3]</sup> Attractive features of SERS include high sensitivity, excellent photostability (no photobleaching), use of a single laser source, multiplexing capability and high signal-to-noise ratio. Another added advantage is that red to near-infrared (NIR) laser wavelengths, which minimizes the problem of interference due to auto fluorescence arising from cells and tissues, can be used for SERS.<sup>[4]</sup> SERS relies on the inelastic interaction of a photon with an analyte. The inherent weakness of the Raman signal intensity is enhanced using a metallic surface.<sup>[5]</sup> Electromagnetic enhancement of the SERS signal arises due to excited electrons of metallic nanoparticles (NPs) oscillating in resonance with the incident optical field making a localized surface plasmon resonance (LSPR).<sup>[6]</sup> Whereas,

chemical enhancement of the signal is the result of charge transfer between the molecule and support surface. SERS nanotags are commonly composed of a noble roughened metallic support surface (usually gold or silver) and an organic dye reporter molecule (RM).<sup>[4,7]</sup> Another important component of a successful nanotag is the aggregating agent, generally an inorganic salt, which reduces the Columbic repulsion energy between the RM and the metallic surface, allowing their tight bonding for molecular finger printing.<sup>[8]</sup> An ideal RM usually has a high Raman scattering cross section, a small number of atoms, molecular symmetry, signal stability and a surface-seeking group. It has been documented recently that the introduction of hetero atoms into the RM facilitates the tight binding to the surface and excludes the requirement of an aggregating agent.<sup>[9]</sup> Another important aspect is the introduction of a second functional group, such as carboxylic acid for direct bioconjugation.

Even though the RM is an important part of a nanotag, its role has not been explored as

comprehensively that of the metallic NPs. However, recently various classes of organic compounds have been rationally designed and tested for their usefulness as new RMs. Graham and co-workers, for example, introduced benzotriazole derivatives for use as dyes in surface-enhanced resonance scattering with silver colloids.<sup>[10]</sup> Maiti et al.<sup>[11]</sup> have reported cyanine and triphenylmethane covalently bound to the gold surface. Lambert and co-workers designed and synthesized new RMs based on alkyne moieties and used them for tissue imaging.<sup>[12]</sup> Highly sensitive probes based on chalcogenopyrylium were published by Harmsen et al.<sup>[13]</sup> The rational design, supported by density functional theory (DFT) calculations of rhodamine with thiol groups at the xanthene ring, has been reported by Brem and Schlücker.<sup>[14]</sup> The above work highlights the importance of the design and synthesis of new RMs with desired structural features and unique fingerprints for selected analytical applications.

Boron complexes constitute versatile fluorescent dyes, and their distinct properties include ease of synthesis, structural modification, stability and compatibility with the biological system as probes. The configuration of this class can readily be controlled through the tuning of the ligands. The scarcity of examples of the boron complexes as RMs for SERS nanotags is mainly due to their low aqueous solubility and lower affinity for the metal surface. However, pyridine, the first molecule that was used for the discovery of SERS,<sup>[15]</sup> and the recent reports on the potential and applications of the boron dipyrromethene compounds (BODIPYs) as SERS nanotags inspired us to design and synthesize a new class of boron complexes based on pyridine-pyrazole ligands, and further test their normal Raman spectra and the potential as RMs for sensitive SERS nanotags.<sup>[16–19]</sup>

## 2 | EXPERIMENTAL

### 2.1 | Materials

All chemicals were purchased from Sigma-Aldrich, Australia unless otherwise stated. BODIPY FL NHS (BDP FL NHS) ester was purchased from Lumiphore. Water was obtained from a Milli-Q plus system (Millipore Co.), and resistivity was reported to be  $\geq 18$  M $\Omega$ .cm. Unless otherwise noted, all chemicals were used without further purification. The solvent tetrahydrofuran (THF) used for the synthesis of 1,3-diketones was first dried with a molecular sieve (4 Å) and was stored under an argon atmosphere for 72 h before using. All reactions were carried out under an inert atmosphere of argon.

### 2.2 | Methods

The progress of each reaction was monitored by thin layer chromatography (TLC) analysis. High-resolution mass spectra (HRMS) were recorded with an Agilent 6538 Q-TOF with dual electrospray ionization (Supporting Information) source. <sup>1</sup>H and <sup>13</sup>C nuclear magnetic resonance (NMR) spectra were recorded on a Bruker Avance spectrometer 400 (<sup>1</sup>H) and 100 MHz (<sup>13</sup>C) in CDCl<sub>3</sub> (de-acidified by passing it through calcium carbonate before use) and with dimethyl sulfoxide (DMSO). NMR and HRMS data are supplied as Supporting Information. Ultraviolet (UV)–visible absorption spectra were recorded on an Agilent Cary Eclipse UV–visible spectrophotometer. A portable Raman microscope (IM-52 Snowy Range, 407 S. 2nd Street Laramie, WY 82070) with 785-nm laser excitation and laser power of 100 mW was used for the Raman analyses.

### 2.3 | Synthesis

Methyl picolinate used for the synthesis of 1,3-diketones was synthesized according to a reported method.<sup>[20]</sup> The synthesis and characterization of the 1,3-diketones: 1-phenyl-3-(pyridine-2-yl) propane-1,3-dione (B<sub>1</sub>), 1-(4-bromophenyl)-3-(pyridine-2-yl) propane-1,3-dione (B<sub>2</sub>), 1-(4-methoxyphenyl)-3-(pyridine-2-yl) propane-1,3-dione (B<sub>3</sub>) and 1-(pyridine-2-yl)-3-(pyridine-4-yl) propane-1,3-dione (B<sub>4</sub>); the pyridine-pyrazole ligands: 2-(3-phenyl-1H-pyrazol-5-yl) pyridine (C<sub>1</sub>), 2-(3-(4-bromophenyl)-1H-pyrazol-5-yl) pyridine (C<sub>2</sub>), 2-(3-(4-methoxyphenyl)-1H-pyrazol-5-yl) pyridine (C<sub>3</sub>) and 2-(3-(pyridin-4-yl)-1H-pyrazol-5-yl) pyridine (C<sub>4</sub>); and the pyridine-pyrazole boron complexes: 2-(5-phenyl-1H-pyrazol-3-yl) pyridine boron complex (P<sub>1</sub>), 2-(3-(4-bromophenyl)-1H-pyrazol-5-yl) pyridine boron complex (P<sub>2</sub>), 2-(3-(4-methoxyphenyl)-1H-pyrazol-5-yl) pyridine boron complex (P<sub>3</sub>), and 2-(3-(pyridin-4-yl)-1H-pyrazol-5-yl) pyridine boron complex (P<sub>4</sub>) are given in the Supporting Information.

### 2.4 | Normal Raman spectra of boron complexes in solid state

To measure Raman spectra of a compound, it was ground to fine powder, a thin layer of which was spread evenly over a microscope slide, and the spectrum collected with an integration time of 0.5 s and 10 accumulations.

## 2.5 | Adsorption of boron complex on AuNPs

P<sub>4</sub> (Mol. Wt. 387.17 g/mol) (0.1 mg,  $0.26 \times 10^{-3}$  M) was dissolved in DMSO (1 mL). The resulting stock solution was used for serial dilutions, using 10  $\mu$ L of the stock solution and diluting it with DMSO (90  $\mu$ L) and using the second dilution as stock for the next and so on till ( $0.26 \times 10^{-9}$  M) was reached. Each solution was poured into a separate vial with 1 mL of AuNPs (see Supportign Information for the preparation method). The vials were rotated overnight using a rotator operating at 300 rpm to mix the two components. The solutions were then centrifuged at 7,000 rpm for 5 min, and the supernatant was discarded carefully without disturbing the bottom AuNPs layer to remove excess P<sub>4</sub> molecules. The residue was suspended in Milli-Q water (1 mL) and was shaken well and sonicated then centrifuged under same conditions. The same process was repeated three times to remove DMSO to avoid signals from the solvent. Finally, boron complexes with AuNPs were obtained, and the adsorption was confirmed by measuring the UV-vis absorption spectrum of every resulting solution.

## 2.6 | Preparation of the standard Raman reporter solution

### 2.6.1 | Boron dipyrromethene FL NHS (BDP FL NHS) solutions

BDP FL NHS boron complex (Mol. Wt. 389.16 g/mol) (0.1 mg,  $0.26 \times 10^{-3}$  M) was dissolved in Milli-Q water (1 mL). Serial dilution was performed to get the desired concentration and each one adsorbed on AuNPs, as described above.

### 2.6.2 | Pyridine solutions

Pyridine (Mol. Wt. 79.10 g/mol) was prepared (0.2 mg,  $0.26 \times 10^{-3}$  M) in Milli-Q water (10 mL). Serial dilution was performed to get the desired concentration and each one adsorbed on AuNPs as described above.

## 2.7 | SERS analysis

The Raman spectra of the boron complexes and standards were recorded in aqueous solution, with a portable Raman microscope (IM-52 Snowy Range) with 785-nm laser excitation and the laser power of 100 mW. The spectra were collected at an integration time of 0.5 s and 10 accumulations.

## 2.8 | Computational method

Gaussian-16 analytical software<sup>[21]</sup> was used for the quantum chemical DFT calculations. The pyridine derivative (P<sub>4</sub>) structure was fully optimized using Becke three hybrid exchange and the Lee–Yang–Parr correlation functional<sup>[22,23]</sup> B3LYP and a Pople split valence diffused and polarized 6-311++G(d,p) basis set. The vibrational frequencies and the Raman activities were calculated on the optimized structure. Vibrational band assignments were made using the Gauss view 6.0.16 molecular visualization programme.<sup>[24]</sup> All calculations were carried out in the gas phase.

## 3 | RESULTS AND DISCUSSION

### 3.1 | Synthesis and characterization

Previous reports have established that pyridine-pyrazolate ligands can be easily synthesized and tuned with a tendency to bind with boron. Based on previously documented literature methods, synthesis of pyridyl pyrazolate boron complexes was carried out via 1,3-diketone pathways (Figure 1).

Various ligands were synthesized using protocols reported in the literature. Selected ketones were treated with an ester in an inert atmosphere using sodium hydride (NaH) in dry THF. The products of the reactions were purified by column chromatography on silica gel and suitable combination of organic solvents as eluents. <sup>1</sup>H NMR studies revealed that the products existed in keto-enolic tautomeric forms, with the enolic form being the dominant. 1,3-Diketones were used to prepare the pyridine-pyrazolate ligands by reacting them with excess hydrazine. These ligands were, in turn, mixed without further purification with BPh<sub>3</sub> in toluene resulting in the boron complexes. All the final complexes were characterized by NMR (<sup>1</sup>H and <sup>13</sup>C) and HRMS (see Supporting Information). All the synthesized boron complexes are new except P<sub>1</sub>, which was synthesized according to a reported method.<sup>[25]</sup>

### 3.2 | Raman spectroscopy (solid-state experimental, DFT based and aqueous solution)

A preliminary investigation of the Raman activity of the synthesized boron complexes was done utilizing normal Raman spectroscopy in the solid state. The Raman profiles of all compounds were quite similar due to the similarity in the compounds' molecular structures (P<sub>1</sub>–P<sub>4</sub>). All

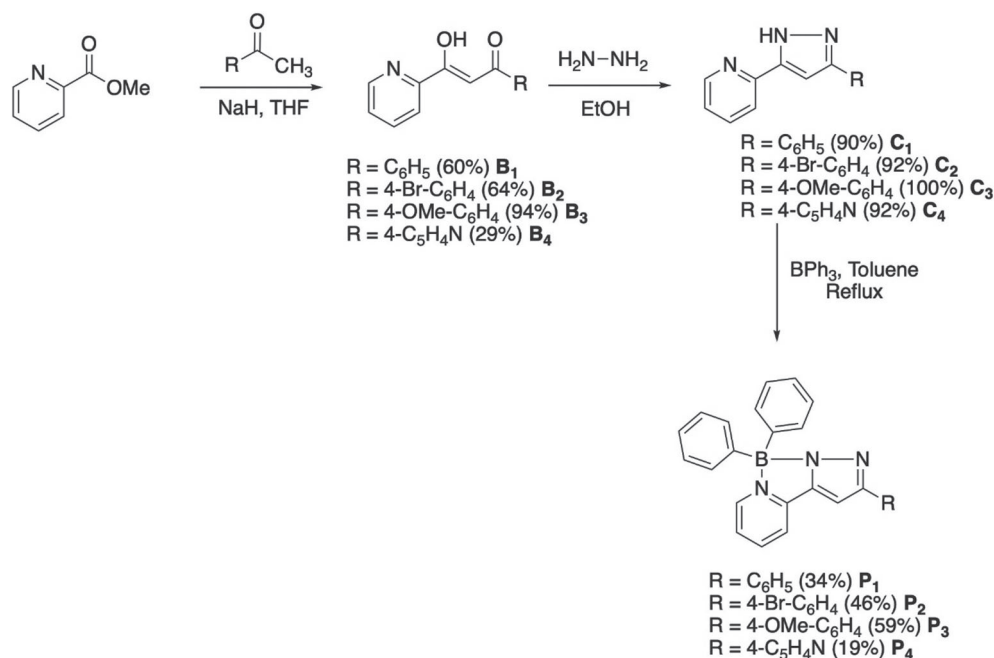


**FIGURE 1** Schematic route for the synthesis of pyridine-pyrazolate boron complexes

the compounds along with their Raman spectra, DFT calculations and DFT(B3LYP)/6-31++G(d,p) optimized structure are depicted in Figure 2a,b, respectively.

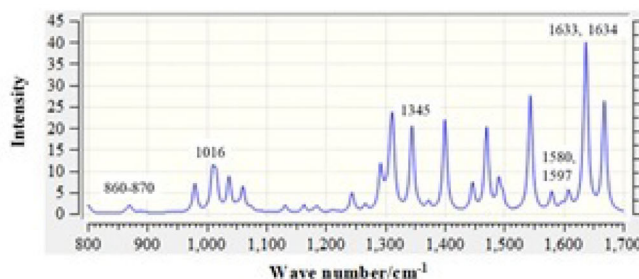
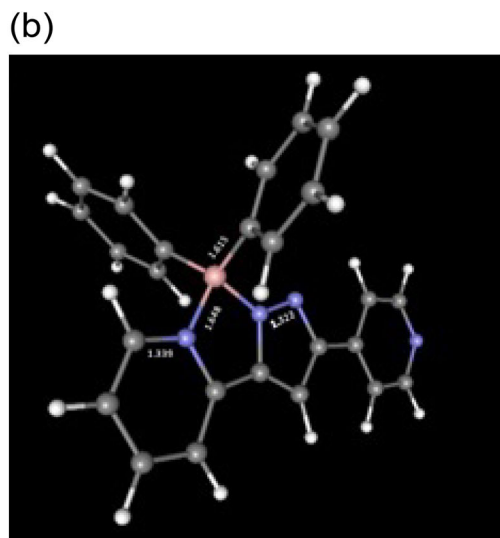
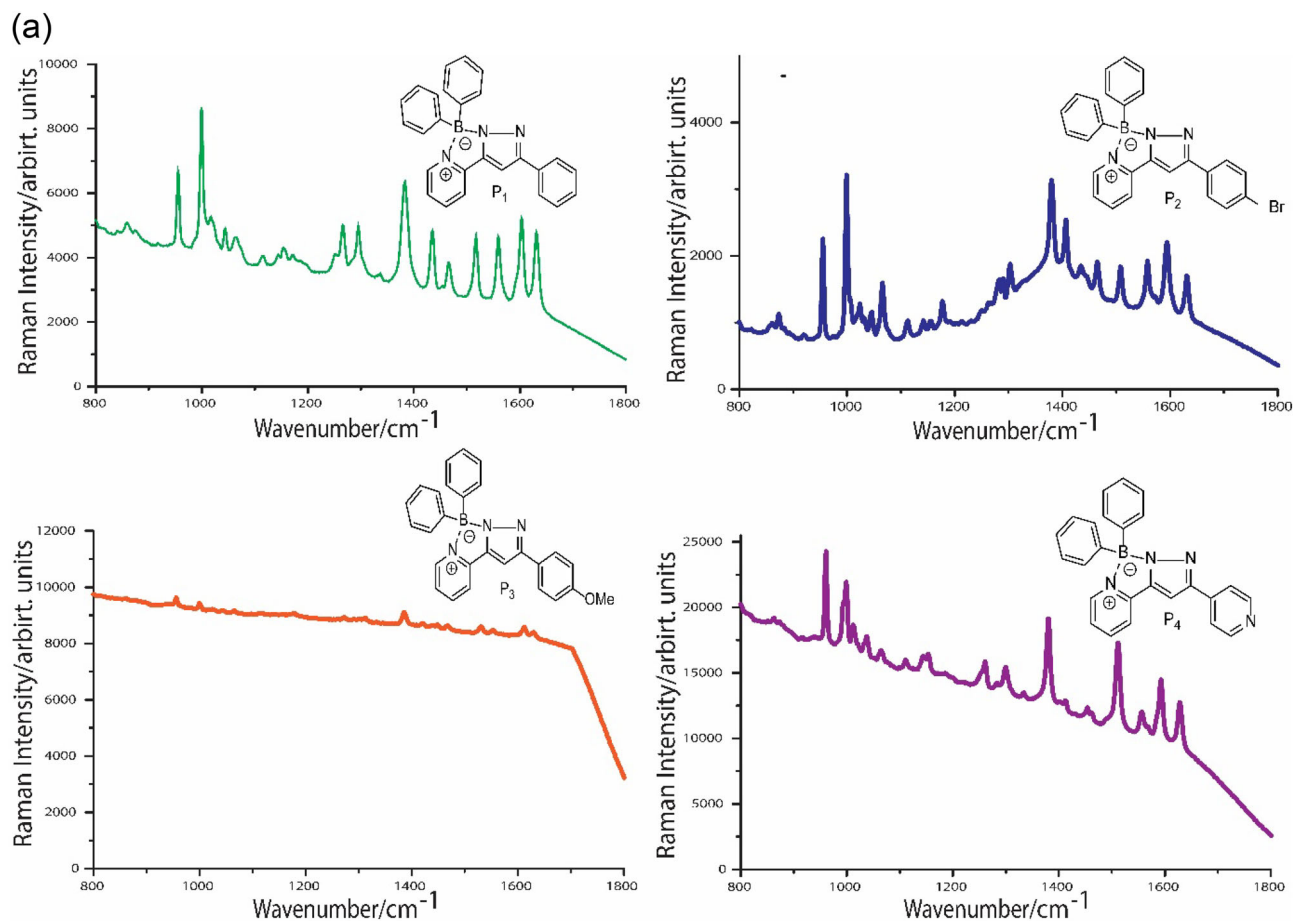
**P**<sub>1</sub>, **P**<sub>2</sub> and **P**<sub>4</sub> exhibited strong Raman signatures. A possible reason for **P**<sub>3</sub>'s poor performance could be the presence of a *p*-OMe group that favours strong fluorescence thus depressing the Raman signals. Although the Raman signal of **P**<sub>3</sub> was weak, the vibrational peaks at 1,000, 1,380 and 1,610  $\text{cm}^{-1}$  were still observable, which were attributed to the vibrational modes of aromatic  $\nu_{\text{C-H}}$ ,  $\nu_{\text{N-N}}$  and  $\nu_{\text{C=N}}$ , respectively.

Among all the tested compounds, the pyridine derivative (**P**<sub>4</sub>) exhibited the most intense Raman spectral profile. The major Raman peaks obtained, along with peak assignments, are presented in Table 1. Given that **P**<sub>4</sub> exhibited well-resolved signals and structural features including nitrogen for attachment to the metal surface, it was chosen for more detailed analysis. The solution Raman spectrum of the bare RM (**P**<sub>4</sub>) was also recorded in 1% DMSO/ $\text{H}_2\text{O}$ , for comparison. Only weak Raman signals were observed for **P**<sub>4</sub> in solution (Figure 3b).

DFT calculations of gas-phase **P**<sub>4</sub> (i.e., no intermolecular hydrogen bonding) were compared with the experimental solid-state data. The DFT(B3LYP)/6-311++G(d,p) calculated frequencies only differ slightly from these experimentally determined values. The  $\text{C=N}$  stretch, which is mixed with  $\text{C=C}$ ,  $\text{C-C}$  and  $\text{C-N}$  stretches, showed a weak peak in the calculated Raman spectrum and a strong one in the experiment. However, strong calculated peaks are apparent at slightly higher energy (1,633, 1,634 and 1,637  $\text{cm}^{-1}$ ) corresponding to a mix of  $\text{C-C}$  and  $\text{C=C}$  stretches.

### 3.3 | SERS analysis

AuNPs of size 40 nm were adopted in this work. The selected dye **P**<sub>4</sub> ( $0.26 \times 10^{-3}$  M) was mixed with AuNPs freshly prepared as described in the Supporting Information. The mixture was shaken well overnight allowing the maximum adsorption of **P**<sub>4</sub> to occur through chemisorption and physisorption. Strong bonding between the RM and support surface was through the nitrogen of the pyridine side chain resulting in N–AuNP bonding as well as electrostatic interactions due to partial positive charges on the pyridine nitrogen and partial negative charge on boron as a result of dative bond formation. Although the nitrogen atoms in the pyrazole provide a potential binding site for AuNPs besides pyridine, they are sterically hindered due to presence of bulky phenyl groups (Figure 2b). Moreover, molecular rearrangements during adsorption process cannot be ignored. More conclusive evidence came from the shifting of distinctive peaks 1,610–1,593  $\text{cm}^{-1}$  arising from  $\text{C=N}$  stretching while N–N stretching (1,380  $\text{cm}^{-1}$ ) was unchanged after adsorption endorsing the fact that the pyridine is participating in electron sharing (Supporting Information—Figure A2.37). It retained its properties even after exposure to a laboratory environment for a few weeks. It is important to note that no aggregating agent was needed for the adsorption of the RM to the surface. The confirmation of adsorption was made through the measurement of optical properties of the AuNPs and AuNPs/RM solutions. The UV–visible absorption of freshly prepared AuNP samples indicated

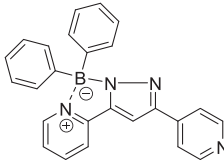


**FIGURE 2** (a) Structure and solid-state Raman spectra of compounds (P<sub>1</sub>–P<sub>4</sub>) with 785-nm laser excitation and laser power of 100 mW. (b) The DFT(B3LYP)/6-31++G(d,p) optimized structure and the calculated Raman spectrum of P<sub>4</sub>

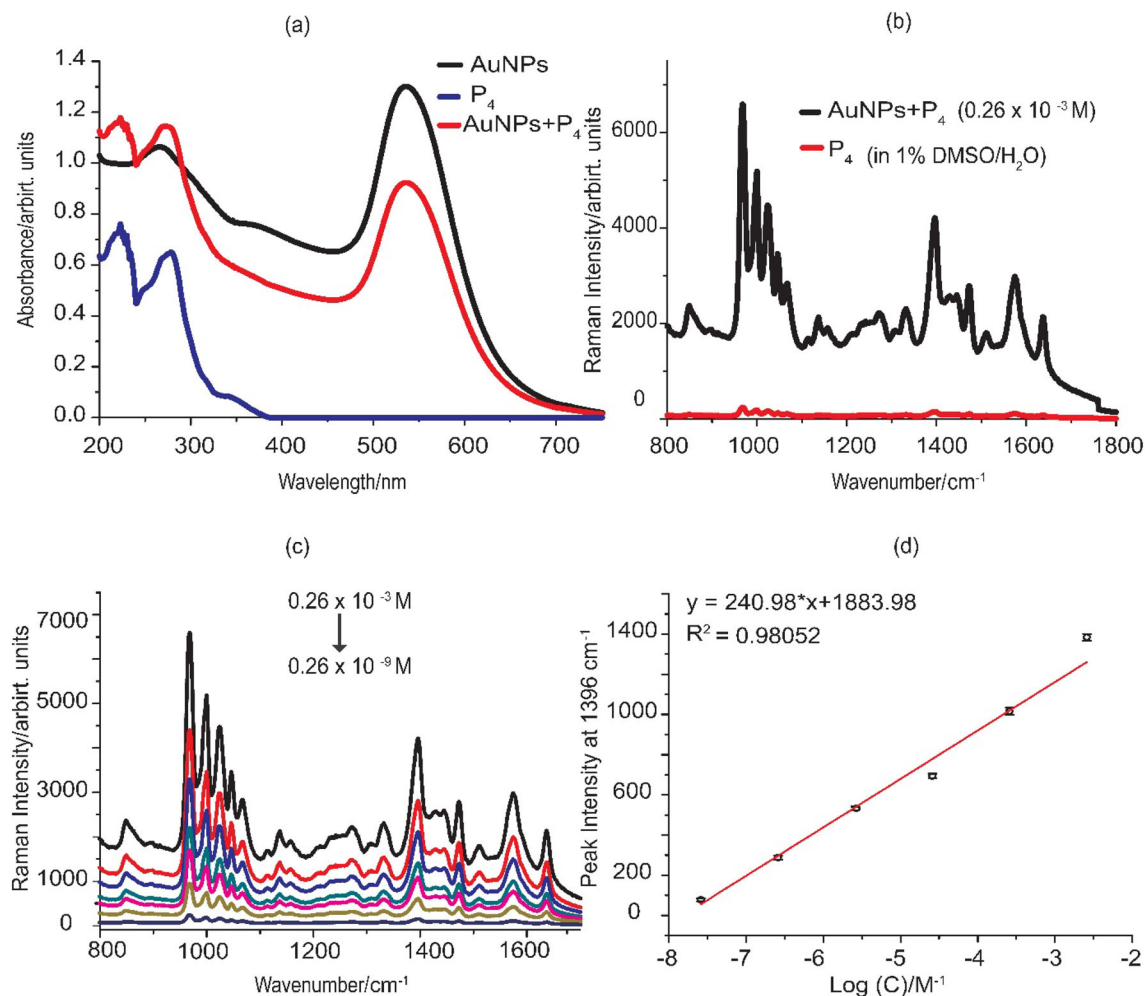
the distinct peak at 536 nm, assigned to the AuNPs due to their LSPR. After the adsorption of the RM, a red shift was observed with the peak value moving to 555 nm (Figure 3a). The typical cross section for

Raman scattering is  $10^{-30}$  cm<sup>2</sup>/sr with surface-enhanced Raman cross section about  $10^{-26}$  cm<sup>2</sup>/sr as reported for the typical Raman dye molecules (e.g., rhodamine 6G and crystal violet).<sup>[26]</sup> Thus, the

**TABLE 1** Chemical structure and major vibrational modes of P<sub>4</sub> in solid state together with the corresponding DFT(B3LYP)/6-311++G (d,p) calculated gas-phase values

| Chemical structure  | $\nu$ (cm <sup>-1</sup> ) (experimental) | $\nu$ (cm <sup>-1</sup> ) (calculated) | Mode of vibration and relative Raman intensity |
|---|--|--|--|
|  | 860                                      | 864, 866                               | Aromatic C-H wagging (w)                       |
|   | 1,000                                    | 1,015, 1,016                           | Aromatic ring breathing (s)                    |
|   | 1,380                                    | 1,345                                  | N-N stretching (s)                             |
|   | 1,610                                    | 1,580, 1,597                           | C=N stretching (s)/(w)                         |

Note: s = strong; w = weak.

**FIGURE 3** (a) Absorption spectra of P<sub>4</sub> adsorbed on AuNPs (red), AuNPs (black) and P<sub>4</sub> (blue) in aqueous media. (b) Raman spectra of bare P<sub>4</sub> in 1% DMSO/H<sub>2</sub>O (red) and P<sub>4</sub>-Au (black) both at 0.26 × 10<sup>-3</sup> M. (c) Concentration-dependent surface-enhanced Raman scattering (SERS) spectra of P<sub>4</sub> to determine the limit of detection. (d) SERS dilution study of P<sub>4</sub> at 1,396 cm<sup>-1</sup>. Error bars represent a standard deviation from three replicates and 10 scans of each with 785-nm laser excitation and exposure time of 0.5 s

Raman cross section of the new developed molecule was estimated about 10<sup>-26</sup> cm<sup>2</sup>/sr. The exact value depends on the excitation frequency and the SERS

substrate. A comparison of SERS spectra for P<sub>4</sub> in aqueous media and with AuNPs demonstrates a significant Raman signal enhancement (Figure 3b).

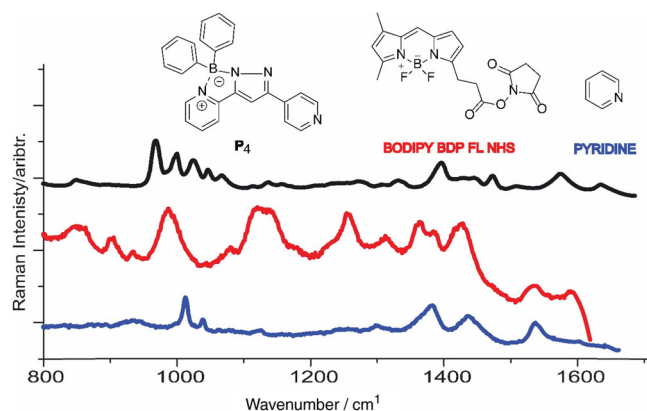


**FIGURE 4** Comparison of surface-enhanced Raman scattering (SERS) spectra of  $P_4$  (black) with BODIPY BDP FL NHS (red) and pyridine (blue) all measured at  $2.6 \times 10^{-8}$  M

### 3.4 | Sensitivity study of the SERS nanotag

A concentration study of  $P_4$  RM was carried out to determine the limit of detection (LOD, Figure 3c). The sharp peak at  $1,396 \text{ cm}^{-1}$  was used to calculate the LOD to be  $0.26 \text{ nM}$  (Figure 3d) by calculating three times the standard deviation of the blank divided by the gradient of the straight line in Figure 3d.

### 3.5 | Comparison with commercial nanotags

Given that  $P_4$  exhibited a sharp Raman signature even at low concentration, it was interesting to compare it with structurally similar and commercially available tag molecules. BODIPY FL NHS (BDP FL NHS) ester was chosen due to structural similarity as both form a five-membered ring complex with boron, which attached via *two* nitrogen atoms. Pyridine was chosen as a conventional second standard because  $P_4$  contains pyridine, which is assumed to be a key part of its interaction with the AuNPs. Even at  $2.6 \times 10^{-8}$  M,  $P_4$  retained a sharp molecular fingerprint whereas the others exhibit broader bands (Figure 4). All had similar intensities.

## 4 | CONCLUSIONS

In summary, we have designed and synthesized a new library of Raman active boron complexes based on pyridine-pyrazole ligands, which have been tuned via substitution. The synthesized compounds were characterized using NMR ( $^1\text{H}$  and  $^{13}\text{C}$ ) and HRMS analysis. The Raman active nature of the compounds under investigation was

evaluated using solid-state normal Raman spectroscopy. The signals of the most Raman active dye were enhanced using 40-nm AuNPs. The dye binding to the AuNPs was strengthened by partial charges on the boron and nitrogen atoms. This resulted in a tight association with the surface and Raman signal enhancement. The SERS effect was found to decrease linearly with concentration upon dilution rendering it useful for quantitative analysis. Further, the LOD was calculated to be  $0.26 \text{ nM}$  at  $1,396 \text{ cm}^{-1}$ . The reported dye retained resolved sharper signals even at this low concentration when compared with structurally similar commercial Raman reporters. The targeted synthesis and ease of molecular tuning with high affinity for AuNPs opens a new window for chemists to develop new RM probes for selected applications. In future, new classes of compounds with distinct molecular signatures and the capability of multiplexing by using secondary functional groups will be synthesized for targeted biological applications.

### ACKNOWLEDGMENTS

This work was funded by the University of Macquarie including a Higher Degree Research Scholarship for RJ.

### ORCID

Rashid Javaid <https://orcid.org/0000-0003-2532-6835>

Nima Sayyadi <https://orcid.org/0000-0002-0044-2170>

Kausala Mylvaganam <https://orcid.org/0000-0002-5226-2833>

Koushik Venkatesan <https://orcid.org/0000-0002-3046-2017>

Yuling Wang <https://orcid.org/0000-0003-3627-7397>

Alison Rodger <https://orcid.org/0000-0002-7111-3024>

### REFERENCES

- [1] N. M. S. Sirimuthu, C. D. Syme, J. M. Cooper, *Anal. Chem.* **2010**, *82*(17), 7369.
- [2] M. Xiao, J. Nyagilo, V. Arora, P. Kulkarni, D. Xu, X. Sun, D. P. Davé, *Nanotechnology* **2009**, *21*(3), 035101.
- [3] M. Li, J. W. Kang, S. Sukumar, R. R. Dasari, I. Barman, *Chem. Sci.* **2015**, *6*(7), 3906.
- [4] Y. Wang, S. Schlücker, *Analyst* **2013**, *138*(8), 2224.
- [5] S., P. L.; D., J. A.; S., N. C.; D., R. P. V, *Annu. Rev. Anal. Chem.* **2008**, *1*(1), 601.
- [6] L. A. Lane, X. Qian, S. Nie, *Chem. Rev.* **2015**, *115*(19), 10489.
- [7] Y. Wang, B. Yan, L. Chen, *Chem. Rev.* **2013**, *113*(3), 1391.
- [8] I. A. Larmour, K. Faulds, D. Graham, *J. Phys. Chem. C* **2010**, *114*(31), 13249.
- [9] M. A. Bedics, H. Kearns, J. M. Cox, S. Mabbott, F. Ali, N. C. Shand, K. Faulds, J. B. Benedict, D. Graham, M. R. Detty, *Chem. Sci.* **2015**, *6*(4), 2302.
- [10] D. Graham, K. Faulds, W. E. Smith, *Chem. Commun* **2006**, *42*, 4363.
- [11] K. K. Maiti, A. Samanta, M. Vendrell, K. S. Soh, M. Olivo, Y. T. Chang, *Chem. Commun.* **2011**, *47*(12), 3514.

- [12] M. Schütz, C. I. Müller, M. Salehi, C. Lambert, S. Schlücker, *J. Biophotonics* **2011**, 4(6), 453.
- [13] S. Harmsen, M. A. Bedics, M. A. Wall, R. Huang, M. R. Detty, M. F. Kircher, *Nat. Commun.* **2015**, 6, 6570.
- [14] S. Brem, S. Schlücker, *J. Phys. Chem. C* **2017**, 121(28), 15310.
- [15] M. Fleischmann, P. J. Hendra, A. J. McQuillan, *Chem. Phys. Lett.* **1974**, 26(2), 163.
- [16] M. Zhao, Y. Xu, M. Xie, L. Zou, Z. Wang, S. Liu, Q. Zhao, *Adv. Healthcare Mater.* **2018**, 7(18), 1800606.
- [17] N. Adarsh, A. N. Ramya, K. K. Maiti, D. Ramaiah, *Chem. – Eur. J.* **2017**, 23(57), 14286.
- [18] M. Yilmaz, M. Erkartal, M. Ozdemir, U. Sen, H. Usta, G. Demirel, *ACS Appl. Mater. Interfaces* **2017**, 9(21), 18199.
- [19] V. I. Kukushkin, N. M. Ivanov, A. A. Novoseltseva, A. S. Gambaryan, I. V. Yaminsky, A. M. Kopylov, E. G. Zavyalova, *PLoS ONE* **2019**, 14(4), e0216247.
- [20] V. Mamane, E. Aubert, Y. Fort, *J. Org. Chem.* **2007**, 72(19), 7294.
- [21] K. I. Peterson, D. P. Pullman, *J. Chem. Educ.* **2016**, 93(6), 1130.
- [22] A. D. Becke, *J. Chem. Phys.* **1993**, 98(7), 5648.
- [23] C. Lee, W. Yang, R. G. Parr, *Phys. Rev. B* **1988**, 37(2), 785.
- [24] P. Kolar, J. Classen, S. G. Hall, *Data Brief* **2019**, 26, 104356.
- [25] W. Zheng, X. M. Pan, L. L. Cui, Z. M. Su, R. S. Wang, *J. Mol. Struct-Theochem.* **2007**, 809(1), 39.
- [26] S. A. Meyer, E. C. L. Ru, P. G. Etchegoin, *J. Phys. Chem. A* **2010**, 114(17), 5515.

### SUPPORTING INFORMATION

Additional supporting information may be found online in the Supporting Information section at the end of this article.

**How to cite this article:** Javid R, Sayyadi N, Mylvaganam K, Venkatesan K, Wang Y, Rodger A. Design and synthesis of boron complexes as new Raman reporter molecules for sensitive SERS nanotags. *J Raman Spectrosc.* 2020;1–8. <https://doi.org/10.1002/jrs.6020>